MASTER THESIS

Resonant Transport with an Interaction in Mesoscopic Systems

メゾスコピック系における相互作用のある共鳴伝導

Keita Sasada

笹田啓太

(35102017)

Department of Physics,
Graduate School of Science and Engineering,
Aoyama Gakuin University

Supervisors: Kenn Kubo and Naomichi Hatano
指導教官：久保健・羽田野直道

2003

論　文　要　旨
（和　文）

提 出 年 度： 2003
提　出　日： 2004/02/25
専　　攻： 物理学
学 生 番 号： 35102017
学 生 氏 名： 笹田啓太
研究指導教員： 久保健・羽田野直道

（論文題目）

メゾスコピック系における相互作用のある共鳴伝導

（内容の要旨）

メゾスコピックな素子のコンダクタンスには、共鳴散乱現象が大きく関わっている。本研究の目的は、共鳴散乱状態の固有値と固有関数を数値計算することにより、多体問題を考慮した量子効果のあるコンダクタンスを算出することである。

共鳴状態は、素子に導線を接続した開いた系に特徴的に現れる。このとき系 Ω の内部にある伝導電子の固有値の期待値の虚部は、恒等式

$$\Im\langle\psi|H|\psi\rangle_{\Omega} = -\frac{\hbar}{2m}\Re\langle\psi|\hat{p}|\psi\rangle_{\partial\Omega}$$

を満たす。この恒等式は、固有値の期待値の虚部が閉曲面 $\partial\Omega$ から流出する流束に等しいことを示している。そのため、粒子の出入りのある系は、極限 $\Omega\to\infty$ で一般的に複素固有値 $E \equiv E_r - iE_i$ を持つ。

同時に、共鳴散乱の固有関数は、ポテンシャルより十分遠方で複素波数 $k = k_r - i\kappa$ を持つ平面波である。つまりこの固有関数は、指数関数的に発散する外向波 $\varphi(x) \propto e^{ik|x|} = e^{\kappa|x|}e^{ik_r|x|}$ である。そのため、有限系でしか扱うことのできない数値計算では、共鳴状態の固有値を算出することは困難である。また、素子内にある局在電子との相互作用を考慮した多体問題を扱うためには、転送行列法等を用いることができないために、更なる困難が伴う。

そこで、本研究では、この開いた系と多体問題を同時に解決する新しい方法として、グリーン関数 $G(E)$ の最小特異値による擬スペクトルから共鳴状態の固有値分布を算出する方法を提案する：

$$\|G(E)\| = \left\|\left(E - H_{\mathbf{eff}}(E)\right)^{-1}\right\|.$$

このとき、導線の効果を表す自己エネルギー $\Sigma(E)$ が複素数であるために、有効ハミルトニアン

$$H_{\mathbf{eff}}(E) = H_{\mathbf{c}} + \Sigma(E) + H_{\mathbf{s-d}}$$

が非エルミート行列になるので、この新しい計算方法が必要となる。なお、上式の $H_{\mathbf{s-d}}$ は、局在スピンと伝導電子のあいだの *s-d* 交換相互作用の項である。

相互作用の無い場合の一電子共鳴状態の複素固有値 $E = E_r - iE_i$ は、この手法による数値解が厳密解と一致することが確かめられたことを報告する。さらに *s-d* 交換相互作用を考慮することで、局在スピンが共鳴状態に与える効果を議論する。

Academic Year of 2003, Submitted on Feb. 25, 2004

Graduate School of Science and Engineering, Aoyama Gakuin University

Resonant Transport with an Interaction in Mesoscopic Systems

Sasada Keita (35102017)
Department of Physics
Supervisors: Kubo Kenn and Hatano Naomichi

The resonant scattering greatly affects the conductance of mesoscopic systems [1]. The resonant states characteristically appear in open quantum systems such as devices connected to leads. Since the resonant states have only outgoing waves which diverge exponentially away from the potential, it is difficult to calculate the resonant states by numerical computations for finite systems [2]. It is also difficult to treat many-body problems with electron interactions in the device, because we cannot use the transfer-matrix method.

In the present thesis we propose a method of solving both the problems of open systems and many-body interactions. The method is to compute the distribution of resonant eigrnvalues from the "pseudospectrum," or the minimum singular value of the retarded Green's function $G_{\mathbf{c}}^{\mathbf{R}}(E)$ [3];

$$\left\| G_{\mathbf{c}}^{\mathbf{R}}(E) \right\| = \left\| \left(E - H_{\mathbf{eff}}(E) \right)^{-1} \right\|.$$

We need the pseudospectrum because the effective Hamiltonian $H_{\mathbf{eff}}(E)$ includes a non-Hermitain self-energy $\Sigma(E)$ expressing the effect of the leads:

$$H_{\mathbf{eff}}(E) = H_{\mathbf{c}} + H_{\mathbf{sd}} + \Sigma(E),$$

where $H_{\mathbf{sd}}$ is the *s-d* exchange interaction between localized spins and conduction electrons.

We first demonstrate that the complex eigenvalues $E = E_{\mathbf{r}} - iE_{\mathbf{i}}$ of resonant states obtained by the present method agree with the exact solutions. We further discuss the effects of the *s-d* exchange interaction on the conductance.

[1] S. Datta, Electronic Transport in Mesoscopic Systems (Cambridge University Press, Cambridge, 1995).

[2] N. Hatano, Complex eigenvalues and resonant states (2003), unpublished.

[3] M. Embree and L. N. Trefethen, SIAM J. Sci. Comput. **23**, 583 (2001).

MASTER THESIS
Resonant Transport with an Interaction in Mesoscopic Systems

Sasada Keita
(35102017)
Department of Physics,
Graduate School of Science and Engineering,
Aoyama Gakuin University
5-10-1 Fuchinobe, Sagamihara, Kanagawa 229-0006, Japan

Supervisors: Kubo Kenn and Hatano Naomichi

February 25, 2004

Abstract

The resonant scattering greatly affects the conductance of mesoscopic systems. The resonant states characteristically appear in open quantum systems such as devices connected to leads. Since the resonant states have only outgoing waves which diverge exponentially away from the potential, it is difficult to obtain the resonant states by numerical computations for finite systems. It is also difficult to treat many-body problems with electron interactions in the device, because we cannot use the transfer-matrix method.

In the present thesis we propose a method of solving both the problems of open systems and many-body interactions. The method is to compute the distribution of resonant eigenvalues from "the pseudospectrum," or the minimum singular value of the retarded Green function $G^{\mathrm{R}}(E)$;

$$||G^{\mathrm{R}}(E)|| = ||(E - \mathcal{H}_{\mathrm{eff}}(E))^{-1}||.$$

We need the pseudospectrum because the effective Hamiltonian $\mathcal{H}_{\mathrm{eff}}(E)$ includes a non-Hermitian self-energy $\Sigma(E)$ expressing the effect of the leads:

$$\mathcal{H}_{\mathrm{eff}}(E) = \mathcal{H}_{\mathrm{c}} + \mathcal{H}_{\mathrm{sd}} + \Sigma(E),$$

where H_{sd} is the s-d exchange interaction between localized spins and conduction electrons.

We first demonstrate that the complex eigenvalues $E = E_{\mathrm{r}} - iE_{\mathrm{i}}$ of resonant states obtained by the present method agree with the exact solution. We further discuss the effects of the *s-d* exchange interaction on the conduction electrons.

Contents

1 Introduction **4**

2 The conductance of mesoscopic systems **5**

3 The phenomenon of resonant scattering **7**
3.1 The origin of complex eigenvalues 7
3.2 Decay of the particle density and the imaginary part of an eigenvalue 10
3.3 The diverging eigenfunction 12
3.4 Problems of calculating the resonant states 12

4 Non-Hermitian Hamiltonian with the self-energy **13**
4.1 What is the self-energy? 13
4.2 Calculation of non-Hermitian self-energy 14

5 The pseudospectrum **20**

6 Calculation of the spectrum **21**
6.1 The double delta potential 21
6.2 The rectangular potential 25
6.3 A double Gaussian potential 28

7 Calculation of the conductance **31**

8 The case of many-body problem **33**
8.1 s-d exchange interaction 33

9 Conclusion **34**

A The analysis of eigenvalues of Double delta potential **36**

B The analysis of eigenvalues of Rectangular potential **38**

1 Introduction

The conductance of mesoscopic systems has been studied in recent years both theoretically and experimentally [1]. The resonant transport is one of the most interesting phenomena in mesoscopic systems. The resonant state affects the conductance of a mesoscopic device in its ballistic transport regime. This phenomenon is an intrinsic feature of open systems. The quantum mechanics of open systems, however, has not been developed so much as applicable to the computation of the conductance of mesoscopic systems.

Effects of many-body interactions are also of great interest. For example, the Kondo interaction between conduction electrons and an impurity spin affects the conductance significantly. It is, however, quite difficult to analyze such a many-body problem theoretically and numerically.

In the present thesis, we propose a new method of treating open quantum systems with interactions. The method is free from approximations and applicable to general many-body problems. In Sec. 2, we review the conductance of mesoscopic systems. In Sec. 3, we explain characteristics of both eigenvalues and eigenfunctions of the resonant scattering phenomenon. We show that the resonant state generally has a complex eigenvalue. Because of it, the self-energy, which are introduce in Sec. 4 by reducing the infinite-dimensional lead Hamiltonians, is non-Hermitian. We calculate the self-energy for one-dimension tight binding model. In Sec. 5, we show how to analyze the Hamiltonian with the non-Hermitian self-energy numerically. The new method utilizes "the pseudospectrum." In Sec. 6, we show the results of resonant states for various potentials. These results agree with the exact solutions. In Sec. 7, we show the results of the conductance of the potentials by using the retarded Green's function and the self-energy of leads. We note that the peaks of the nonlinear conductance are caused by the resonant states of a conduction electron. In Sec. 8, we try to discuss many-body problems by using the present new method. In particular, we focus on the s-d exchange interaction. In Sec. 9, concluding remarks are given.

2 The conductance of mesoscopic systems

In the present section, we review the difference in the conductance of macroscopic systems and mesoscopic systems. The mesoscopic system is a system of size much smaller than the mean free path l_m of the electron. Its typical size is several nanometers, containing thousands of atoms or hundreds of molecules. Many phenomena occurring in the mesoscopic system have been applied to the nanotechnology, which has rapidly developed in recent years.

The mesoscopic system behaves very differently from the macroscopic system. One of the most interesting behaviors is the fluctuating dependence of the conductance on the energy of the conduction electrons (Fig. 1). The conductance G of the macroscopic system follows Ohm's law:

$$G = \sigma W/L, \tag{1}$$

where σ is the conductivity, L is the length of the system, and W is the width of the system. The conductance of the mesoscopic system, on the other hand, is given by the Landauer formula:

$$G = \frac{2e^2}{h} MT(E), \tag{2}$$

where h is the Planck constant, e is the electron charge, M is the number of transverse modes, and $T(E)$ is the energy-dependent transmission function. We see in the above formula that the conductance of the mesoscopic system is proportional to the transmission function. In other words, the conductance is determined purely from the quantum mechanics of conduction electrons.

We present an experimental result of measuring the conductance of a mesoscopic system, the two-dimensional electron gas (2EDG) in GaAs-AlGaAs heterostructures [2]. As the width W of the constriction is reduced, the conductance decreases in discrete steps of height $2e^2/h$ (Fig. 2). This is consistent with what we showed in Eq. (2); M is an integer denoting the number of transverse modes at the Fermi energy. Although the width of the conductor changes continuously, the number of the modes changes discretely. Such a phenomenon happens only in mesoscopic systems, where the system size is less than the mean free path l_m.

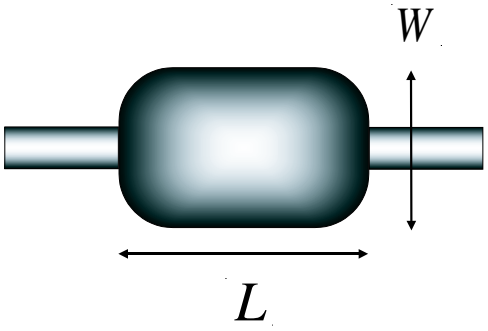

(a)

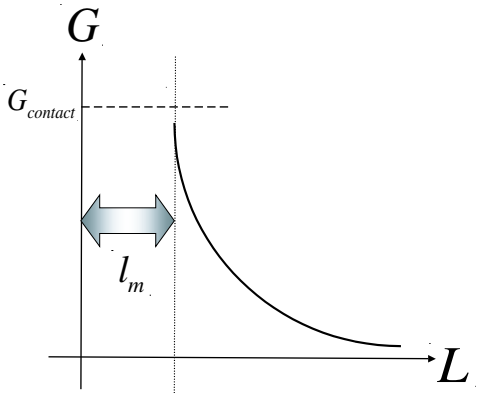

(b)

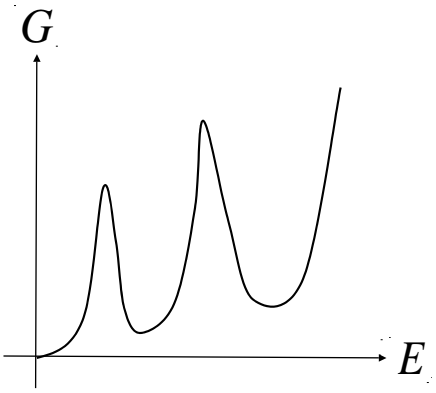

(c)

Figure 1: (a) A conductor of length L and width W. (b) The conductance G is inversely proportional to the length of the conductor for $L \gg l_m$. In the region $L \ll l_m$, however, the conductance reaches a limit, namely the contact conductance G_{contact}, and is independent of L. (c) In the latter region, the conductance shows an fluctuating dependence on the electron energy.

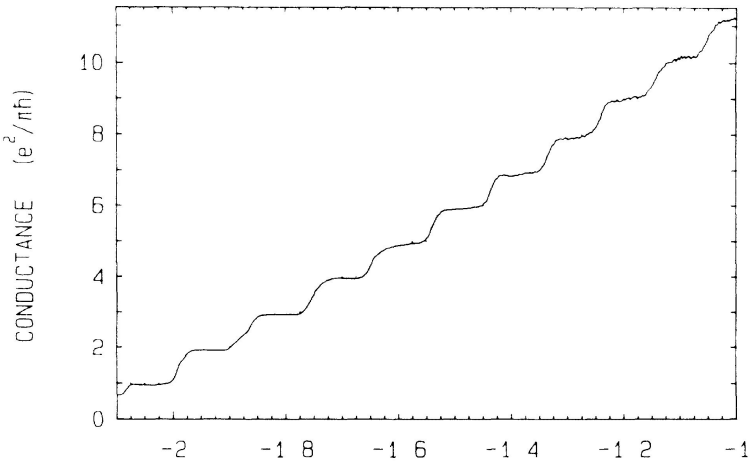

Figure 2: A quantized conductance of the ballistic region (from Ref. [2]). The transverse axis denotes the gate voltage and the perpendicular axis denotes the measured conductance.

3 The phenomenon of resonant scattering

In the present section, we explain the phenomenon of resonant scattering. Let us consider conduction electrons travelling in a mesoscopic device with two leads (Fig. 3). We put a conduction electron into the device through one lead. The incident electron is reflected again and again by the confining potential of the mesoscopic device, and thus stays in the conductor for a while. After some time, the electron may go out through the other lead. This is the classical picture of resonant transport. This transport differs greatly from the normal transport, because the transport has a characteristic time (namely the lifetime) of the electron's stay in the device.

The device itself is an open system, because the electrons get in and out of it. We show below that the open system generally has complex eigenvalues.

3.1 The origin of complex eigenvalues

In the present section, we show that the resonant state generally has a complex eigenvalue [3]. First, consider the Schrödinger equation

$$\mathcal{H}\psi(\vec{x}) \;=\; E\psi(\vec{x}), \tag{3}$$

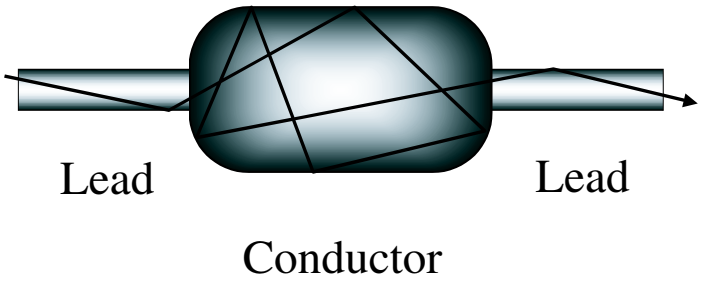

Figure 3: A piece of conductor with two leads attached. In a classical picture, the conduction electron is transported along the arrow.

where the Hamiltonian is given by

$$\mathcal{H} = \mathcal{K} + \mathcal{V}, \tag{4}$$

with

$$\mathcal{K} \equiv \frac{\vec{p}^2}{2m} = -\frac{\hbar^2}{2m}\vec{\nabla}^2, \tag{5}$$

$$\mathcal{V} \equiv V(\vec{x}). \tag{6}$$

The potential energy here is a Hermitian operator: $V(\vec{x})^* = V(\vec{x})$.

We show below that the kinetic energy, on the other hand, is not necessarily a Hermitian operator. For the purpose, we define the expectation value of the Hamiltonian by the integration limited to a volume Ω in the form

$$\langle\psi|\mathcal{H}|\psi\rangle_\Omega \equiv \iiint_\Omega \psi(\vec{x})^* \mathcal{H}\psi(\vec{x}) dV. \tag{7}$$

The reason for introducing the integration volume Ω will be evident below. The expectation value of the kinetic term is transformed owing to Gauss's

theorem as

$$\begin{aligned}\langle\psi|\mathcal{K}|\psi\rangle_\Omega &= -\frac{\hbar^2}{2m}\iiint_\Omega \psi(\vec{x})^*\vec{\nabla}^2\psi(x)dV \\ &= \frac{\hbar^2}{2m}\iiint_\Omega \left(\vec{\nabla}\psi(\vec{x})^*\right)\cdot\left(\vec{\nabla}\psi(\vec{x})\right)dV \\ &- \frac{\hbar^2}{2m}\iint_{\partial\Omega}\psi(\vec{x})^*\vec{\nabla}\psi(\vec{x})\cdot d\vec{S}. \end{aligned} \tag{8}$$

The complex conjugate of Eq. (8) gives

$$\begin{aligned}\left(\langle\psi|\mathcal{K}|\psi\rangle_\Omega\right)^* &= \frac{\hbar^2}{2m}\iiint_\Omega \left(\vec{\nabla}\psi(\vec{x})\right)\cdot\left(\vec{\nabla}\psi(\vec{x})^*\right)dV \\ &- \frac{\hbar^2}{2m}\iint_{\partial\Omega}\psi(\vec{x})\vec{\nabla}\psi(\vec{x})^*\cdot d\vec{S}. \end{aligned} \tag{9}$$

Using Eqs. (8) and (9), we have the imaginary part of the expectation value of the Hamiltonian as follows:

$$\begin{aligned}2i\Im\langle\psi|\mathcal{H}|\psi\rangle_\Omega &= 2i\Im\langle\psi|\mathcal{K}|\psi\rangle_\Omega \\ &= -\frac{\hbar^2}{2m}\iint_{\partial\Omega}\left(\psi(\vec{x})^*\vec{\nabla}\psi(\vec{x}) - \psi(\vec{x})\vec{\nabla}\psi(\vec{x})^*\right)\cdot d\vec{S} \\ &= -\frac{i\hbar}{2m}\iint_{\partial\Omega}\left(\psi(\vec{x})^*\left(\frac{\hbar}{i}\vec{\nabla}\right)\psi(\vec{x}) + \psi(\vec{x})\left(-\frac{\hbar}{i}\vec{\nabla}\right)\psi(\vec{x})^*\right)\cdot d\vec{S} \\ &= -\frac{i\hbar}{2m}\iint_{\partial\Omega}\left(\psi(\vec{x})^*\vec{p}\psi(\vec{x}) + \psi(\vec{x})\left(\vec{p}\psi(\vec{x})\right)^*\right)\cdot d\vec{S} \\ &= -\frac{i\hbar}{m}\Re\iint_{\partial\Omega}\psi(\vec{x})^*\vec{p}\psi(\vec{x})\cdot d\vec{S}. \end{aligned} \tag{10}$$

Thus we arrive at the formula

$$\Im\langle\psi|\mathcal{H}|\psi\rangle_\Omega = -\frac{\hbar}{2m}\Re\langle\psi|p_n|\psi\rangle_{\partial\Omega}, \tag{11}$$

where p_n is the normal component of the momentum on the surface $\partial\Omega$. The left-hand side of Eq. (11) denotes the imaginary part of the expectation value of the Hamiltonian limited to a volume Ω, while the right-hand side of Eq. (11) denotes the expectation of a momentum flux going out of the volume Ω. In other words, the imaginary part of the expectation of the Hamiltonian

indicates a momentum flux out of the volume. By taking the limit $\Omega \to \infty$, we define a complex eigenvalue as

$$E = E_{\rm r} - iE_{\rm i} \equiv \lim_{\Omega\to\infty} \langle\psi|\mathcal{H}|\psi\rangle_\Omega \tag{12}$$

with $E_{\rm i} > 0$. Thus we conclude that a state of an open system generally has a complex eigenvalue. We refer to the complex states as the resonant states.

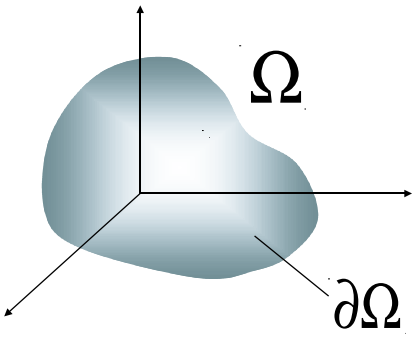

Figure 4: An arbitrary volume Ω and its closed surface $\partial\Omega$.

3.2 Decay of the particle density and the imaginary part of an eigenvalue

In the present subsection, we derive a relation between the imaginary part $E_{\rm i}$ of a resonant eigenvalue and the decay rate of the resonant state. We now consider the time-dependent Schrödinger equation

$$i\hbar\frac{\partial}{\partial t}\Psi(\vec{x},t) = H\Psi(\vec{x},t). \tag{13}$$

We assume a solution of the form of the variable separation:

$$\Psi(\vec{x},t) \;=\; \psi(\vec{x})\phi(t). \tag{14}$$

This gives us a set of equations:

$$i\hbar\frac{d}{dt}\phi(t) \;=\; E\phi(t), \tag{15}$$

$$H\psi(\vec{x}) \;=\; E\psi(\vec{x}). \tag{16}$$

Equation (15) yields a solution of the form

$$\phi(t) = e^{\frac{E}{i\hbar}t} = e^{\frac{E_\mathrm{r}}{i\hbar}t} e^{-\frac{E_\mathrm{i}}{\hbar}t}. \tag{17}$$

Using Eqs. (14) and (17), we obtain the electron density of the form

$$\iiint_\Omega |\Psi(\vec{x},t)|^2 dV = e^{-\frac{2E_\mathrm{i}}{\hbar}t} \langle\psi|\psi\rangle_\Omega. \tag{18}$$

Equation (18) indicates that the electron density in the volume Ω decays exponentially. Thus the quantity $\hbar/2E_\mathrm{i}$ yields the lifetime τ of the resonant state as follows:

$$\tau \equiv \frac{\hbar}{2E_\mathrm{i}}. \tag{19}$$

The lifetime is infinite if the eigenvalue is real, i.e. if $E_\mathrm{i} = 0$.

We see that the imaginary part of the eigenvalue of the resonant state relates the decay rate of the density in a volume to the momentum flux out of the volume. The relation between the two quantities is a very plausible consequence.

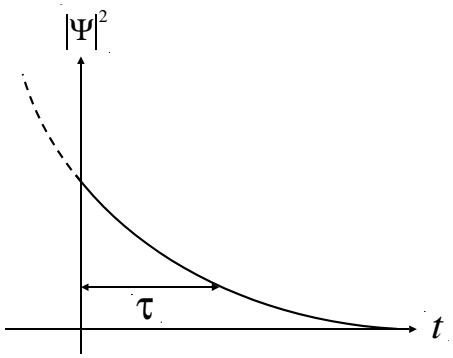

Figure 5: Decay of the particle density in the volume Ω, where τ is the lifetime.

3.3 The diverging eigenfunction

The dispersion relation is given by $E = \hbar^2 k^2 / 2m$ far away from the scattering potential. Hence the resonant state must have a complex wave number

$$k = k_r - i\kappa, \tag{20}$$

where $E_\mathrm{r}, E_\mathrm{i}, k_\mathrm{r}$, and κ are related to each other as follows:

$$\begin{cases} E_\mathrm{r} &= \dfrac{\hbar^2 \left(k_\mathrm{r}^2 - \kappa^2\right)}{2m} \\ E_\mathrm{i} &= \dfrac{\hbar^2 k_\mathrm{r} \kappa}{m}. \end{cases} \tag{21}$$

Here the wave function is, away from the scattering potential, a plane wave with the complex wave number,

$$\psi(\vec{x}) \propto e^{ik_\mathrm{r}|\vec{x}| + \kappa|\vec{x}|}, \tag{22}$$

which is diverging as $|\vec{x}| \to \infty$. Equation (22) indicates that a resonant state has an eigenfunction diverging exponentially away from the potential.

3.4 Problems of calculating the resonant states

We summarize the characteristics of the resonant state in open systems as follows:

- The eigenvalue of the resonant state generally has a complex value;
- The eigenfunction of the resonant state diverges exponentially away from the potential.

Because of these features, it has been difficult to compute the eigenvalue of the resonant state.

4 Non-Hermitian Hamiltonian with the self-energy

In the previous section, we demonstrated that it is difficult to analyze the eigenvalue of the resonant state. We propose a method of solving the problem in the present section.

4.1 What is the self-energy?

The self-energy describes the effect of the leads attached the conductor. This is an important conceptual step; it allows us to replace an infinite open system with a finite system (Fig. 6), thereby to compute the resonant state numerically.

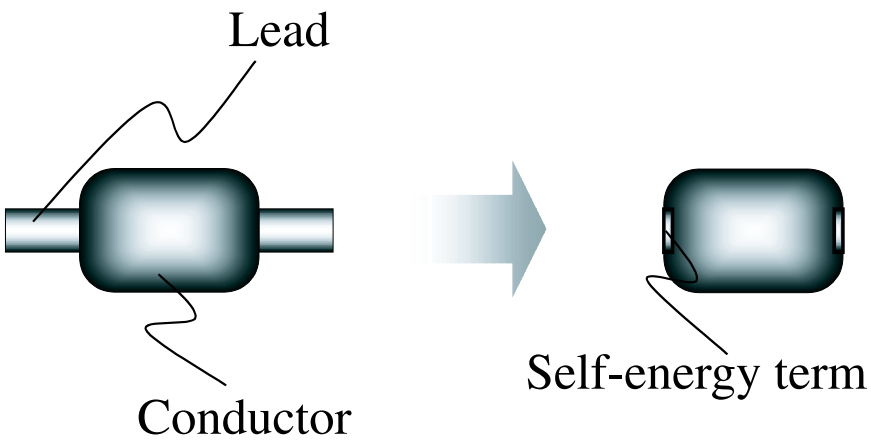

Figure 6: We can reduce a conductor with leads to a conductor with self-energy terms.

4.2 Calculation of non-Hermitian self-energy

In the present section, we show how to calculate the self-energy $\Sigma(E)$. Let us consider the one-dimensional tight-binding model on an infinite lattice as shown in Fig. 7.

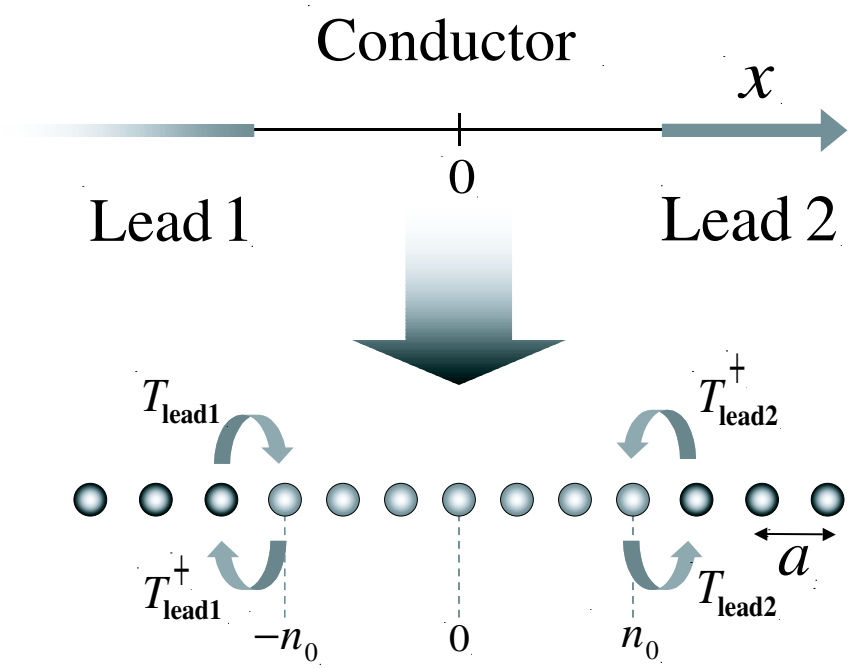

Figure 7: A lattice for the whole system.

The Hamiltonian of the whole system is given by

$$\begin{aligned}\mathcal{H} &= -t\sum_{i=-\infty}^{\infty}\left(c_{i+1}^{\dagger}c_i + c_i^{\dagger}c_{i+1} - 2c_i^{\dagger}c_i\right) + \sum_{i=-n_0}^{n_0} V_i c_i^{\dagger}c_i \\ &= \mathcal{H}_{\rm c} + \mathcal{H}_{\rm lead1} + \mathcal{H}_{\rm lead2} + T_{\rm lead1} + T_{\rm lead}^{\dagger} + T_{\rm lead2} + T_{\rm lead2}^{\dagger}, \qquad (23)\end{aligned}$$

where

$$\mathcal{H}_{\rm c} = -t\sum_{i=-n_0}^{n_0-1}\left(c_{i+1}^{\dagger}c_i + c_i^{\dagger}c_{i+1}\right) + \sum_{i=-n_0}^{n_0-1}\left(V_i + 2t\right)c_i^{\dagger}c_i, \qquad (24)$$

$$\mathcal{H}_{\rm lead1} = -t\sum_{i=-\infty}^{-n_0-2}\left(c_{i+1}^{\dagger}c_i + c_i^{\dagger}c_{i+1}\right) + \sum_{i=-\infty}^{-n_0-2} 2tc_i^{\dagger}c_i, \tag{25}$$

$$\mathcal{H}_{\rm lead2} = -t\sum_{i=n_0+1}^{\infty}\left(c_{i+1}^{\dagger}c_i + c_i^{\dagger}c_{i+1}\right) + \sum_{i=n_0+1}^{\infty} 2tc_i^{\dagger}c_i. \tag{26}$$

$$T_{\rm lead1} = -tc_{-n_0}^{\dagger}c_{-n_0-1}, \tag{27}$$

$$T_{\rm lead1}^{\dagger} = -tc_{-n_0-1}^{\dagger}c_{-n_0}, \tag{28}$$

$$T_{\rm lead2} = -tc_{n_0}^{\dagger}c_{n_0+1}, \tag{29}$$

$$T_{\rm lead2}^{\dagger} = -tc_{n_0+1}^{\dagger}c_{n_0}. \tag{30}$$

The term $\mathcal{H}_{\rm c}$ is the Hamiltonian of the conductor, $\mathcal{H}_{\rm lead1}$ is the Hamiltonian of the lead 1, $\mathcal{H}_{\rm lead2}$ is the Hamiltonian of the lead 2, $T_{\rm lead1}$ is the hopping energy from the lead 1 to the conductor, $T_{\rm lead1}^{\dagger}$ is the hopping energy from the conductor to the lead 1, $T_{\rm lead2}$ is the hopping energy from the lead 2 to the conductor, and $T_{\rm lead2}^{\dagger}$ is the hopping energy from the conductor to the lead 2, whereas t is the hopping energy and V_i is the potential energy on site i. A matrix representation of Eq. (23) is given by

$$\mathcal{H} = \left(\begin{array}{ccc|cccc|ccc}
\ddots & \ddots & \ddots & \ddots & & & & & & \\
\ddots & 2t & -t & 0 & & & & & & \\
\ddots & -t & 2t & -t & 0 & & & & & \\
\hline
\ddots & 0 & -t & V_{-n_0}+2t & -t & & & & & \\
 & & 0 & -t & \ddots & -t & & 0 & & \\
 & & & & -t & V_{n_0}+2t & & -t & 0 & \ddots \\
\hline
 & & & & 0 & -t & & 2t & -t & \ddots \\
 & & & & & 0 & & -t & 2t & \ddots \\
 & & & & & \ddots & & \ddots & \ddots & \ddots
\end{array}\right)$$

$$\equiv \left(\begin{array}{c|c|c}
\mathcal{H}_{\rm lead1} & T_{\rm lead1} & 0 \\
\hline
T_{\rm lead1}^{\dagger} & \mathcal{H}_{\rm c} & T_{\rm lead2} \\
\hline
0 & T_{\rm lead2}^{\dagger} & \mathcal{H}_{\rm lead2}
\end{array}\right). \tag{31}$$

Note that the above Hamiltonian has infinite dimensions. Here we consider the retarded Green's function defined by

$$G^R = \frac{1}{(E+i\eta)\,I - \mathcal{H}} \tag{32}$$

$$= \left(\begin{array}{c|c|c} (E+i\eta)\,I-\mathcal{H}_{\rm lead1} & -T_{\rm lead1} & 0 \\ \hline -T_{\rm lead1}^{\dagger} & (E+i\eta)\,I-\mathcal{H}_{\rm c} & -T_{\rm lead2} \\ \hline 0 & -T_{\rm lead2}^{\dagger} & (E+i\eta)\,I-\mathcal{H}_{\rm lead2} \end{array}\right)^{-1} \quad (33)$$

$$\equiv \left(\begin{array}{c|c|c} G_{\rm lead1} & G_{\rm lead1,c} & 0 \\ \hline G_{\rm c,lead1} & G_{\rm c} & G_{\rm c,lead2} \\ \hline 0 & G_{\rm lead2,c} & G_{\rm lead2} \end{array}\right) \quad (34)$$

Hence we have

$$\left(\begin{array}{c|c|c} (E+i\eta)\,I-\mathcal{H}_{\rm lead1} & -T_{\rm lead1} & 0 \\ \hline -T_{\rm lead1}^{\dagger} & (E+i\eta)\,I-\mathcal{H}_{\rm c} & -T_{\rm lead2} \\ \hline 0 & -T_{\rm lead2}^{\dagger} & (E+i\eta)\,I-\mathcal{H}_{\rm lead2} \end{array}\right) \left(\begin{array}{c|c|c} G_{\rm lead1} & G_{\rm lead1,c} & 0 \\ \hline G_{\rm c,lead1} & G_{\rm c} & G_{\rm c,lead2} \\ \hline 0 & G_{\rm lead2,c} & G_{\rm lead2} \end{array}\right) = I. \quad (35)$$

We obtain from Eq. (35) simultaneous equations as follows:

$$\left\{\begin{array}{lcl} [(E+i\eta)\,I-\mathcal{H}_{\rm lead1}]G_{\rm lead1,c}-T_{\rm lead1}G_{\rm c} &=& 0, \\ -T_{\rm lead1,c}^{\dagger}G_{\rm lead1,c}+[(E+i\eta)\,I-\mathcal{H}_{\rm c}]G_{\rm c}-T_{\rm lead2}G_{\rm lead2,c} &=& I, \\ -T_{\rm lead2}^{\dagger}G_{\rm c}+[(E+i\eta)\,I-\mathcal{H}_{\rm lead2}]G_{\rm lead2,c} &=& 0, \end{array}\right. \quad (36)$$

which is followed by

$$\left\{\begin{array}{lcl} G_{\rm lead1,c} &=& [(E+i\eta)\,I-\mathcal{H}_{\rm lead1}]^{-1}T_{\rm lead1}G_{\rm c}, \\ G_{\rm lead2,c} &=& [(E+i\eta)\,I-\mathcal{H}_{\rm lead2}]^{-1}T_{\rm lead2}^{\dagger}G_{\rm c}. \end{array}\right. \quad (37)$$

Substituting Eq. (37) for the second line of Eq. (36), we can write the retarded Green's function of the conductor in the form

$$\Big([(E+i\eta)\,I-\mathcal{H}_{\rm c}]-T_{\rm lead1}^{\dagger}[(E+i\eta)\,I-\mathcal{H}_{\rm lead1}]^{-1}T_{\rm lead1} - T_{\rm lead2}[(E+i\eta)\,I-\mathcal{H}_{\rm lead2}]^{-1}T_{\rm lead2}^{\dagger}\Big)\,G_{\rm c}=I, \quad (38)$$

or

$$G_{\rm c}(E)=\frac{1}{(E+i\eta)\,I-\mathcal{H}_{\rm eff}(E)}, \quad (39)$$

where the effective Hamiltonian $\mathcal{H}_{\rm eff}(E)$ is given by the self-energy of the lead 1, $\Sigma_{\rm lead1}(E)$, and the self energy of the lead 2, $\Sigma_{\rm lead2}(E)$, as follows:

$$\left\{\begin{array}{lcl} \mathcal{H}_{\rm eff}(E) &\equiv& \mathcal{H}_{\rm c}+\Sigma_{\rm lead1}(E)+\Sigma_{\rm lead2}(E), \\ \Sigma_{\rm lead1}(E) &=& T_{\rm lead1}^{\dagger}\left[(E+i\eta)\,I-\mathcal{H}_{\rm lead1}\right]^{-1}T_{\rm lead1}, \\ \Sigma_{\rm lead2}(E) &=& T_{\rm lead2}\left[(E+i\eta)\,I-\mathcal{H}_{\rm lead2}\right]^{-1}T_{\rm lead2}^{\dagger}. \end{array}\right. \quad (40)$$

Here $T_{\rm lead1}, T^\dagger_{\rm lead1}, T_{\rm lead2}$, and $T^\dagger_{\rm lead2}$ are all semi-infinite matrices.

Let us write down the self-energy of the lead 1, $\Sigma_{\rm lead1}(E)$:

$$\begin{aligned}\Sigma_{\rm lead1}(E) &= \begin{pmatrix} \cdots & 0 & -t \\ & 0 & 0 \\ \iddots & & \vdots \end{pmatrix} \Big(\mathcal{G}_{\rm lead1} \Big) \begin{pmatrix} \vdots & & \iddots \\ 0 & 0 & \\ -t & 0 & \cdots \end{pmatrix} \\ &= t^2 \begin{pmatrix} \mathcal{G}_{\rm lead1}(-n_0,-n_0) & 0 & \cdots & 0 \\ 0 & 0 & & \vdots \\ \vdots & & \ddots & \vdots \\ 0 & \cdots & \cdots & 0 \end{pmatrix}, \end{aligned} \tag{41}$$

where $\mathcal{G}_{\rm lead1}(-n_0,-n_0)$ is the element on the bottom-right corner of the matrix

$$\mathcal{G}_{\rm lead1} \equiv [(E+i\eta) - \mathcal{H}_{\rm lead1}]^{-1}. \tag{42}$$

The self-energy $\Sigma_{\rm lead1}(E)$ here is a $(2n_0+1)\times(2n_0+1)$ matrix. Let us now calculate $\mathcal{G}_{\rm lead1}$, which is the inverse matrix of

$$\begin{aligned}\mathcal{M}^{(0)} &\equiv \mathcal{G}^{-1}_{\rm lead1} = (E+i\eta)\, I - \mathcal{H}_{\rm lead1} \\ &= \begin{pmatrix} \ddots & t & 0 & \vdots \\ t & E-2t+i\eta & t & 0 \\ 0 & t & E-2t+i\eta & t \\ \cdots & 0 & t & E-2t+i\eta \end{pmatrix}. \end{aligned} \tag{43}$$

This is a semi-infinite matrix. In order to invert the matrix, we need to calculate the determinant of $\mathcal{M}^{(0)}$,

$$\det \mathcal{M}^{(0)} \equiv \begin{vmatrix} \ddots & t & 0 & \vdots \\ t & E-2t+i\eta & t & 0 \\ 0 & t & E-2t+i\eta & t \\ \cdots & 0 & t & E-2t+i\eta \end{vmatrix}. \tag{44}$$

The element on the bottom-right corner of $\mathcal{G}_{\rm lead1}$ is given by

$$\mathcal{G}_{\rm lead1}(-n_0,-n_0) = \frac{\det \mathcal{M}^{(1)}}{\det \mathcal{M}^{(0)}} \equiv X, \tag{45}$$

where the matrix $\mathcal{M}^{(1)}$ is given by removing the bottom row and the rightmost column of the matrix $\mathcal{M}^{(0)}$:

$$\mathcal{M}^{(1)} \equiv \left(\begin{array}{ccc|c} \ddots & t & 0 & \\ t & E-2t+i\eta & t & \\ 0 & t & E-2t+i\eta & \\ \hline & & & \end{array}\right). \tag{46}$$

We now note that the cofactor expansion of Eq. (44) with respect to the bottom row yields

$$\det \mathcal{M}^{(0)} \;=\; (E-2t+i\eta)\det \mathcal{M}^{(1)} - t^2 \det \mathcal{M}^{(2)}, \tag{47}$$

where the matrix $\mathcal{M}^{(n)}$ is given by removing the bottom n rows and the rightmost n columns of the matrix $\mathcal{M}^{(0)}$. Assuming that the ratio of the determinants must be equal to each other,

$$X \equiv \frac{\det \mathcal{M}^{(1)}}{\det \mathcal{M}^{(0)}} = \frac{\det \mathcal{M}^{(2)}}{\det \mathcal{M}^{(1)}} = \frac{\det \mathcal{M}^{(3)}}{\det \mathcal{M}^{(2)}} = \cdots, \tag{48}$$

we have from Eq. (47) the following equation for X:

$$\frac{1}{X} \;=\; (E-2t+i\eta) - t^2 X. \tag{49}$$

The solutions of Eq. (49) are

$$\mathcal{G}_{\mathrm{lead1}}(-n_0,-n_0) \;\equiv\; X = \frac{E-2t+i\eta \pm i\sqrt{4t^2-(E-2t+i\eta)^2}}{2t^2}. \tag{50}$$

The "retarded" Green's function must satisfy the condition

$$\Im \mathcal{G}_{\mathrm{lead1}} < 0; \tag{51}$$

thus we choose the minus sign in Eq. (50). Taking the limit $\eta \to 0$ in Eq. (50), we arrive at the self-energy term of the lead 1:

$$\Sigma_{\mathrm{lead1}}(E) \;=\; \begin{pmatrix} \frac{E-2t-i\sqrt{4t^2-(E-2t)^2}}{2} & 0 & \cdots & 0 \\ 0 & 0 & & \vdots \\ \vdots & & \ddots & \vdots \\ 0 & \cdots & \cdots & 0 \end{pmatrix}. \tag{52}$$

In the same way, the self-energy of the lead 2 is given by

$$\Sigma_{\text{lead2}}(E) = \begin{pmatrix} 0 & \cdots & \cdots & 0 \\ \vdots & \ddots & & \vdots \\ \vdots & & 0 & 0 \\ 0 & \cdots & 0 & \frac{E-2t-i\sqrt{4t^2-(E-2t)^2}}{2} \end{pmatrix}. \quad (53)$$

Thus the effective Hamiltonian of the conductor is given by

$$\mathcal{H}_{\text{eff}}(E) = \mathcal{H}_c + \Sigma(E), \quad (54)$$

with

$$\begin{cases} \mathcal{H}_c & = -t \sum_{i=-n_0}^{n_0} \left(c_{i+1}^\dagger c_i + c_i^\dagger c_{i+1} \right) + \sum_{i=-n_0}^{n_0} \left(V_i + 2t \right) c_i^\dagger c_i, \\ \Sigma(E) & = \dfrac{E-2t-i\sqrt{E\left(4t-E\right)}}{2} \sum_{\text{edge}} c_{\text{edge}}^\dagger c_{\text{edge}}. \end{cases}$$

The matrix representation of Eq. (54) is

$$\mathcal{H}_{\text{eff}}(E) = \begin{pmatrix} V_{-n_0} + 2t + \frac{E-2t-i\sqrt{E(4t-E)}}{2} & -t & \cdots & 0 \\ -t & \ddots & \ddots & 0 \\ \vdots & \ddots & \ddots & -t \\ 0 & 0 & -t & V_{n_0} + 2t + \frac{E-2t-i\sqrt{E(4t-E)}}{2} \end{pmatrix}. \quad (55)$$

This effective Hamiltonian has two characteristics as follows:

- Non-Hermitian;
- E-dependent.

We cannot easily diagonalize this effective Hamiltonian due to the above features.

5 The pseudospectrum

To compute the eigenvalue distribution of the effective Hamiltonian Eq. (54), we introduce the pseudospectrum in the present section. Trefethen recently pointed out that the so-called pseudospectrum of non-symmetric matrices is suitable for calculating eigenvalues of the matrices [4]. There are several definitions of the pseudospectrum. Throughout the thesis, A is an $N \times N$ matrix, and $\Lambda(A)$ denotes its spectrum, i.e., its eigenvalues, a subset of the complex plane $\mathbf{C}$. The pseudospectrum of A is a nested subset of $\mathbf{C}$ that expands to fill the complex plane as $\epsilon \to \infty$.

> Definition. For each $\epsilon \geq 0$, the ϵ-pseudospectrum $\Lambda_\epsilon(A)$ of A is the set of numbers $z \in \mathbf{C}$ satisfying any of the following equivalent conditions:
> (i) $|| \, (z - A)^{-1} \, || \geq \epsilon^{-1}$;
> (ii) $\sigma_{\min}(z - A) \leq \epsilon$;
> (iii) $||Au - zu|| \leq \epsilon$ for some vector u with $||u|| = 1$;
> (iv) z is an eigenvalue of $A + E$ for some matrix E with $||E|| \leq \epsilon$.

Here $\sigma_{\min}$ denotes the minimum singular value, and we employ the convention that $|| \, (z - A)^{-1} \, || = \infty$ for $z \in \Lambda(A)$.

We obtain the resonant eigenvalues from the minimum singular value as follows. We calculate the norm of the retarded Green's function:

$$||G^{\mathrm{R}}(E)|| = || \, (E - \mathcal{H}_{\mathrm{eff}}(E))^{-1} \, || = \sigma_{\min} \, (E - \mathcal{H}_{\mathrm{eff}}(E))^{-1} \, . \tag{56}$$

A complex value E for which Eq. (56) diverges indicates a resonant eigenvalue. In other words, we seek a region where the minimum singular value of the inverse matrix of the retarded Green's function $G^{\mathrm{R}}(E)$ satisfies

$$\sigma_{\min} \, (E - \mathcal{H}_{\mathrm{eff}}(E)) \leq \epsilon, \tag{57}$$

where ϵ is a small positive number.

6 Calculation of the spectrum

In the present section, we calculate the resonant eigenvalues and their eigenfunctions for several types of the potential.

6.1 The double delta potential

We consider a finite potential well shown in Fig. 8,

$$V(x) = V_0 \left(\delta(x+d) + \delta(x-d)\right) \tag{58}$$

where $V_0 > 0$.

We use the pseudospectrum to obtain the eigenvalues for the double delta potential. Choosing the unit of $\hbar^2/2m = 1$, we calculated the minimum singular value (57) in the case $V_0 = 1$ and $d = 10$. The distribution of $\sigma_{\min}(E)$ is shown in Fig. 9. The estimates of ten resonant eigenvalues are shown in Fig. 10. The corresponding ten resonant eigenfunctions are shown in Fig. 11.

Both eigenvalues and eigenfunctions of the resonant states obtained by the present new method agree with the exact solutions described in Appendix A. Thus we confirm that the present method yields the exact solution.

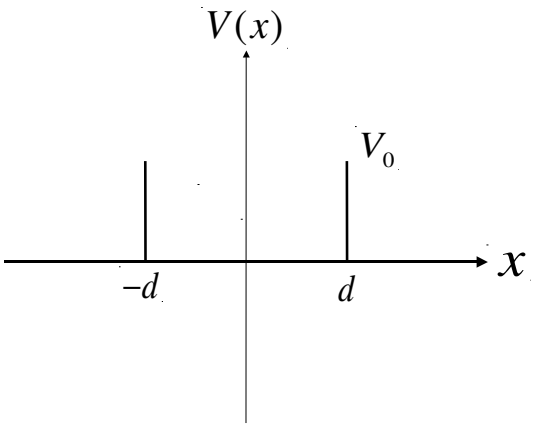

Figure 8: The double delta potential.

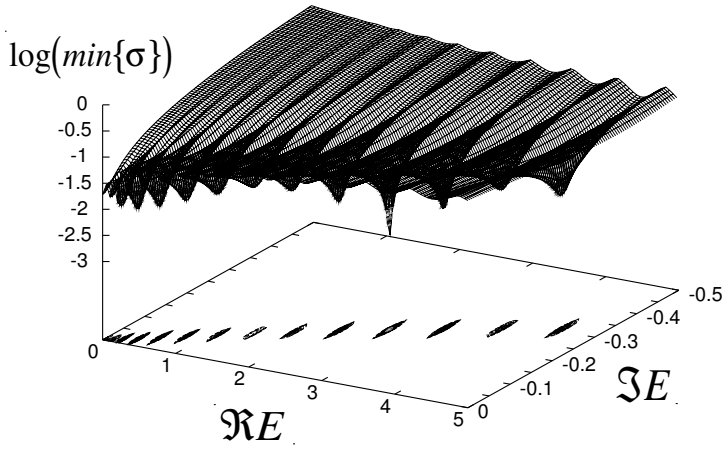

Figure 9: The distribution of the minimum singular value for the double delta potential (58).

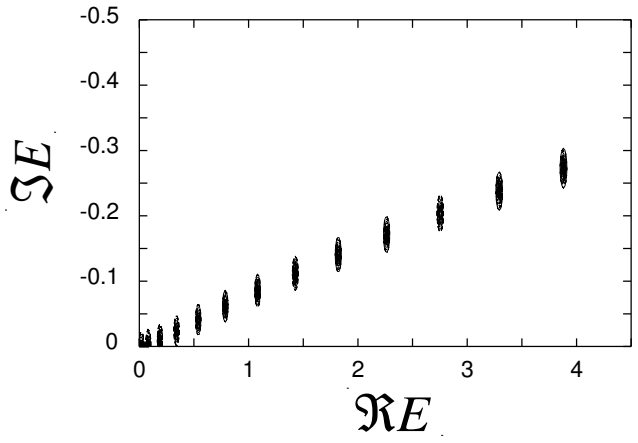

Figure 10: The pseudospectrum for the double delta potential (58).

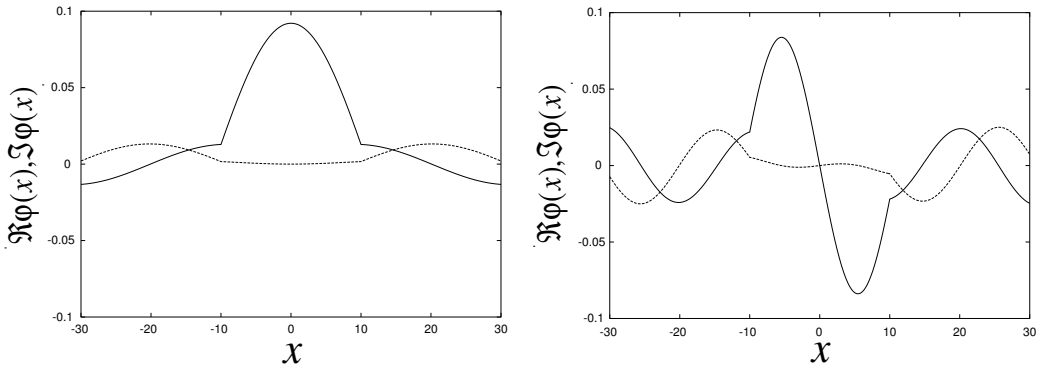
$\Re\varphi(x),\Im\varphi(x)$
x

(a)

$\Re\varphi(x),\Im\varphi(x)$
x

(b)

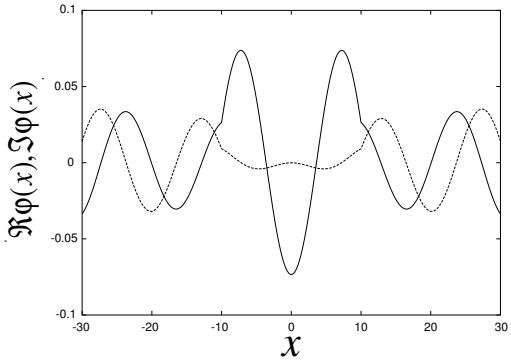
$\Re\varphi(x),\Im\varphi(x)$
x

(c)

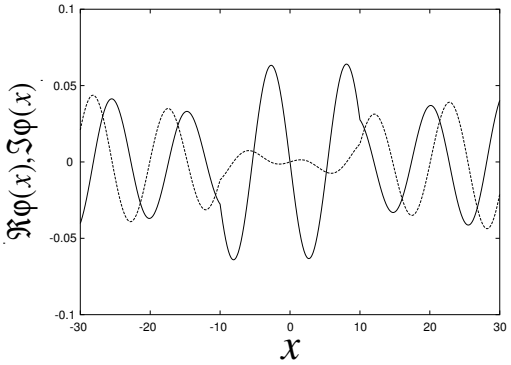
$\Re\varphi(x),\Im\varphi(x)$
x

(d)

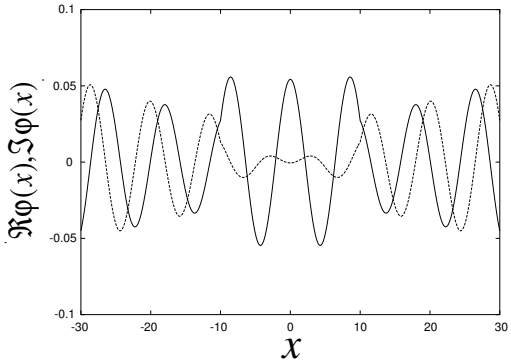
$\Re\varphi(x),\Im\varphi(x)$
x

(e)

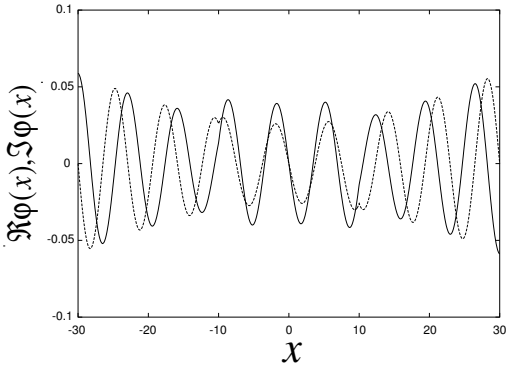
$\Re\varphi(x),\Im\varphi(x)$
x

(f)

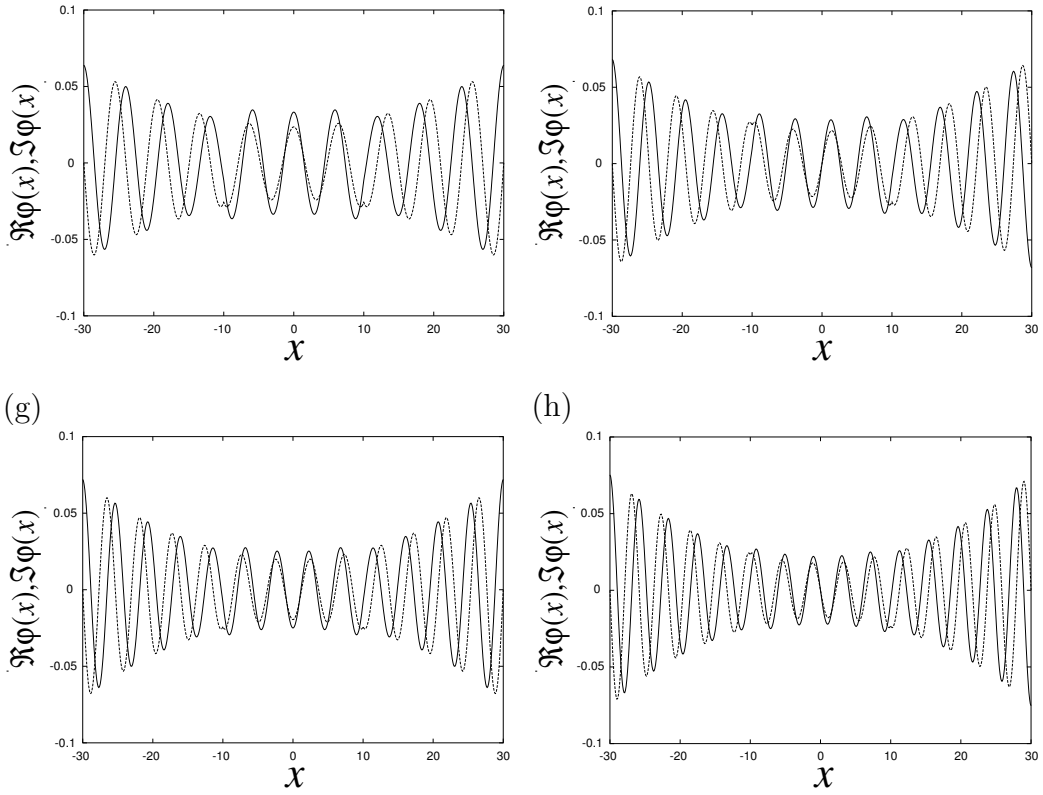

Figure 11: The resonant outgoing waves for the double delta potential (58). The solid lines indicate the real part of the resonant waves $\Re\phi(x)$, and the dotted lines indicate the imaginary part $\Im\phi(x)$. We can see that these waves diverge exponentially away from the potential. (a) The first resonant state $E = 0.020473 - 0.000515i$. (b) The second resonant state $E = 0.082756 - 0.003827i$. (c) The third resonant state $E = 0.188836 - 0.011573i$. (d) The forth resonant state $E = 0.340713 - 0.024093i$. (e) The fifth resonant state $E = 0.539820 - 0.040984i$. (f) The sixth resonant state $E = 0.787001 - 0.061622i$. (g) The seventh resonant state $E = 1.082703 - 0.085415i$. (h) The eighth resonant state $E = 1.427135 - 0.111870i$. (i) The ninth resonant state $E = 1.820373 - 0.140594i$. (j) The tenth resonant state $E = 2.262408 - 0.171275i$.

6.2 The rectangular potential

Next, we consider a finite potential barrier shown in Fig. 12,

$$V(x) = \begin{cases} 0 & (|x| > d) \\ V_0 & (|x| \leq d) \end{cases} \tag{59}$$

where $V_0 > 0$.

We use the pseudospectrum to obtain the eigenvalues for the rectangular potential. Choosing the unit of $\hbar^2/2m = 1$, we calculated the minimum singular value (57) in the case $V_0 = 1$ and $d = 1$. Its distribution is show in Fig. 13. The estimates of the first two eigenvalues are shown in Fig. 14. The corresponding two eigenfunctions and their squared moduli are shown in Fig. 15. Both eigenvalues and eigenfunctions of the resonant state obtained by the present new method agree with the exact solutions described in Appendix B.

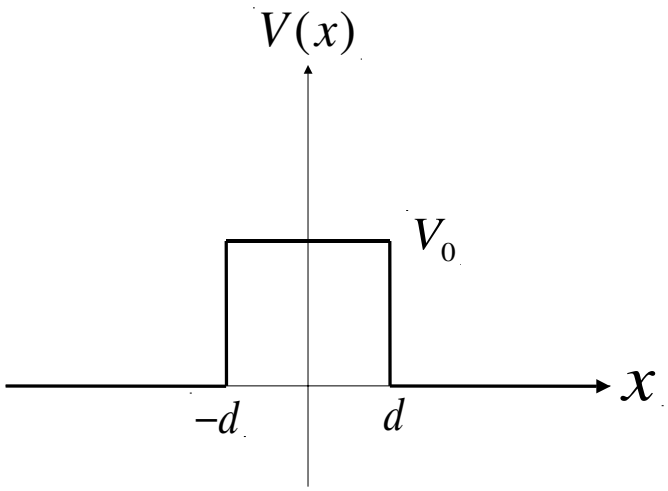

Figure 12: The rectangular potential.

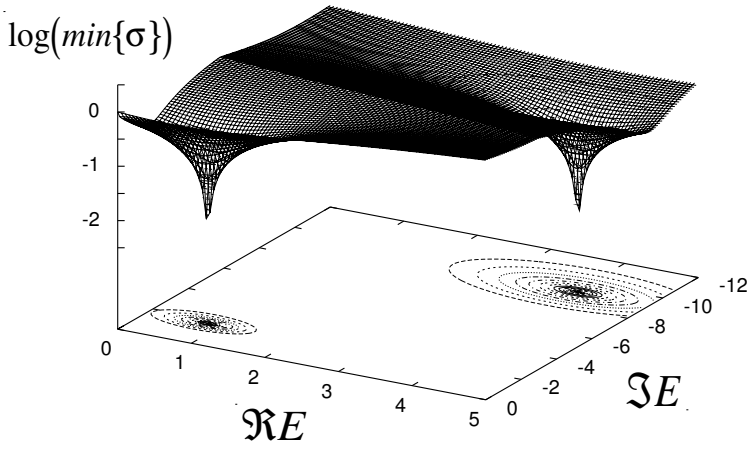

Figure 13: The distribution of the minimum singular value for the rectangular potential (59).

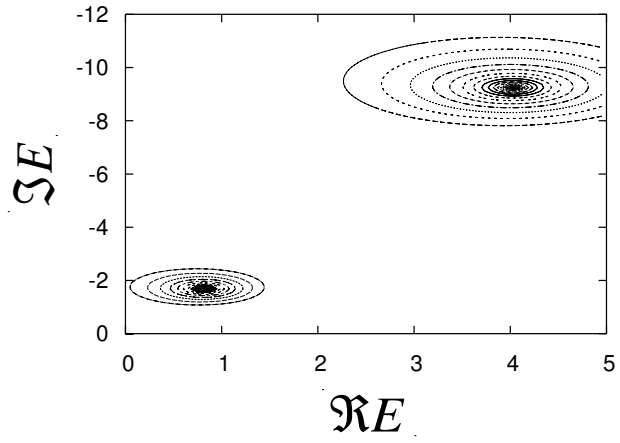

Figure 14: The pseudospectrum for the rectangular potential (59).

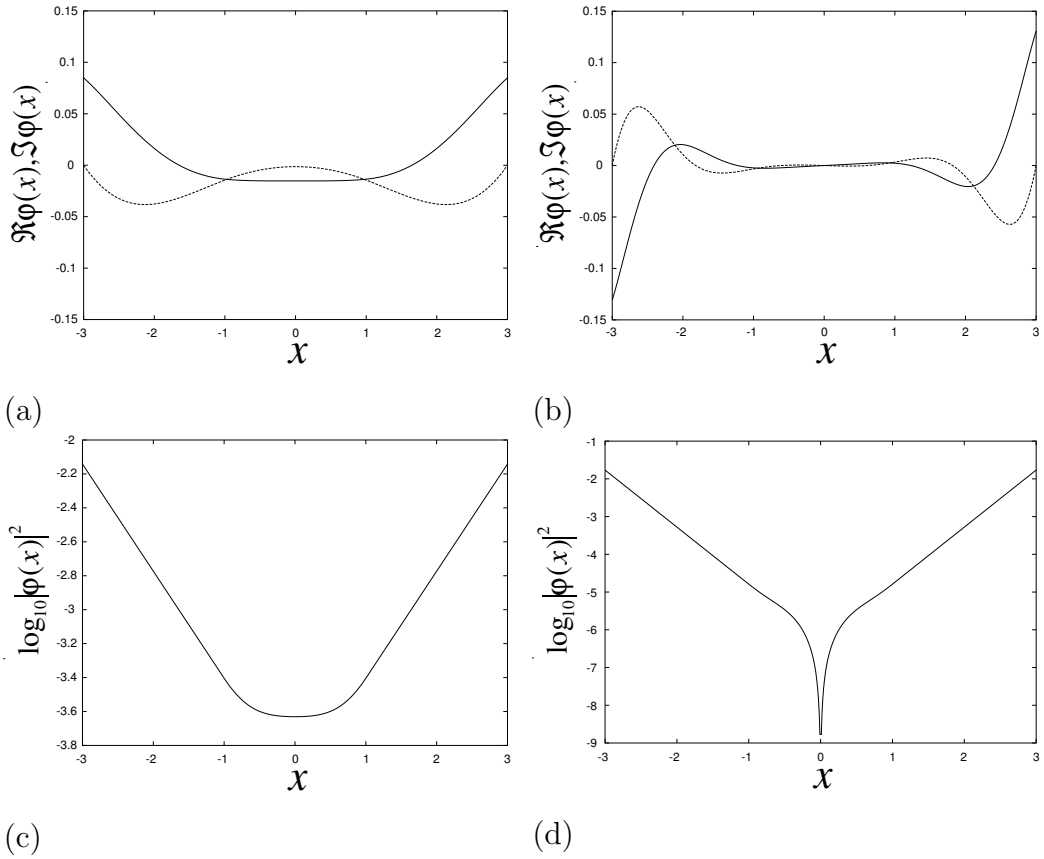

Figure 15: The resonant outgoing waves for the rectangular potential (59). In (a) and (b), the solid lines indicate the real part of resonant waves, $\Re\phi(x)$ and the dotted lines indicate the imaginary part, $\Im\phi(x)$. (a) The first resonant state $E = 0.821201 - 1.688081i$. (b) The second resonant state $E = 4.030598 - 9.245670i$. (c) The squared modulus for the first resonant state. (d) The squared modulus for the second resonant state.

6.3 A double Gaussian potential

Finally, we consider a finite potential shown in Fig. 16,

$$V(x) = 2e^{-(x/3)^2} - 3e^{-x^2}. \tag{60}$$

Choosing the unit of $\hbar^2/2m = 1$, we calculated the minimum singular value (57) for this potential. Its distribution is shown in Fig. 17. The estimates of the first two eigenvalues are shown in Fig. 18. The corresponding two eigenfunctions and their squared moduli are shown in Fig. 19.

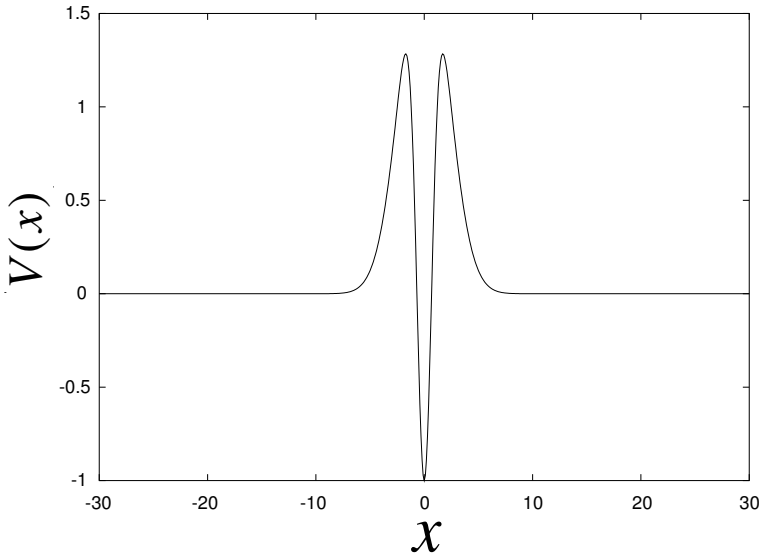

Figure 16: The double gaussian potential.

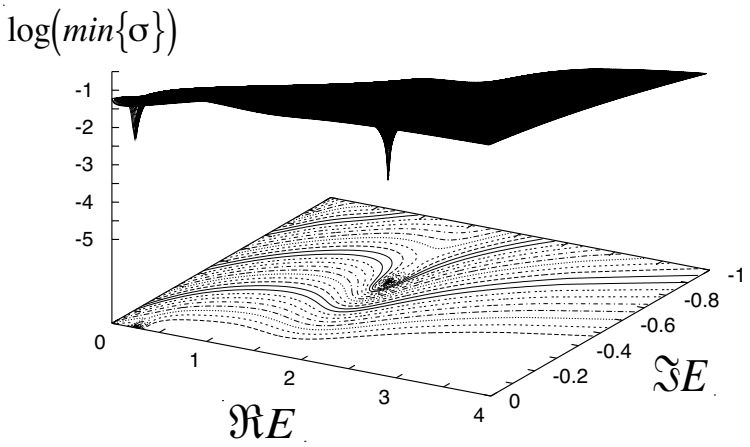

Figure 17: The distribution of the minimum singular value for the double Gaussian potential (60).

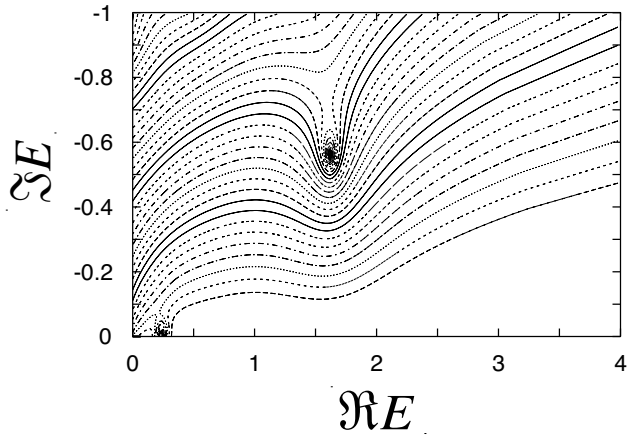

Figure 18: The pseudospectrum for the double Gaussian potential (60).

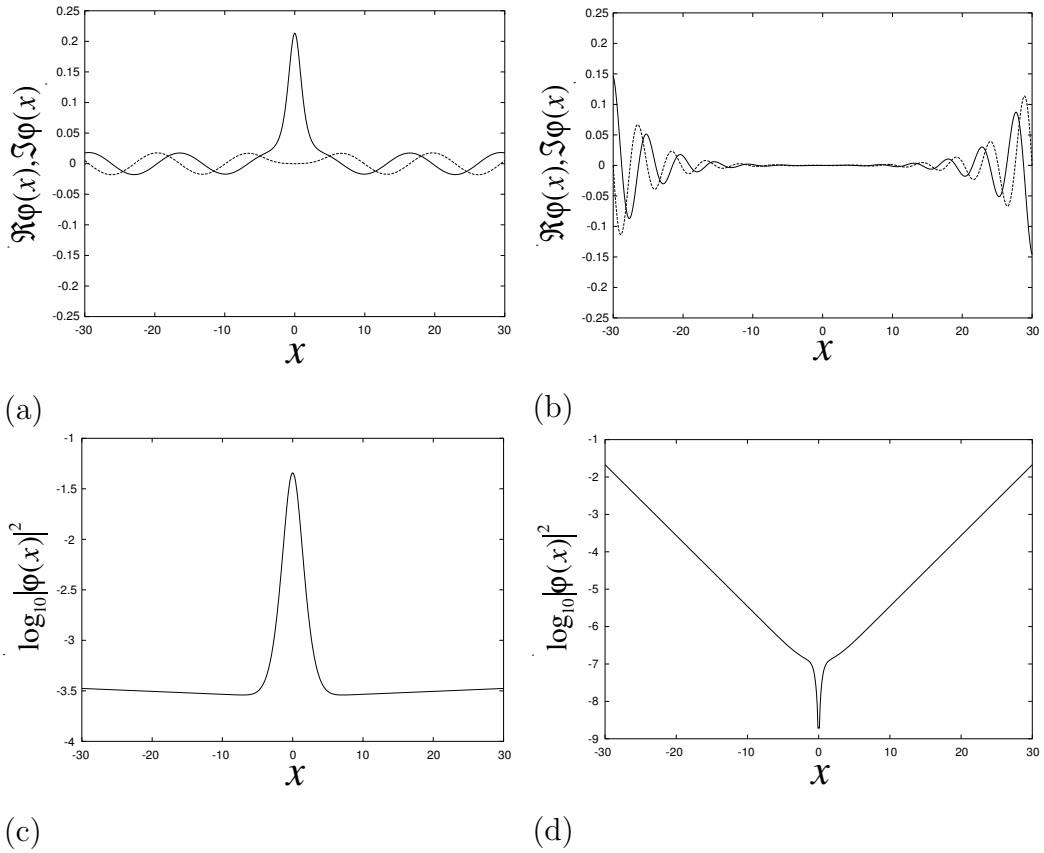

Figure 19: The resonant outgoing waves for the double gaussian potential (60). In (a) and (b), the solid lines indicate the real part of resonant waves, $\Re\phi(x)$, and the dotted lines indicate the imaginary part, $\Im\phi(x)$. We can see that these waves diverge exponentially away from the potential. (a) The first resonant state $E = 0.233484 - 0.003228i$. (b) The second resonant state $E = 1.620332 - 0.561901i$. (c) The squared modulus of the first resonant state. (d) The squared modulus of the second resonant state.

7 Calculation of the conductance

In the present section, we calculate the conductance from the retarded Green's function of a conductor with the self-energy of both the lead 1 and the lead 2. We can write a transmission function from the lead 1 to the lead 2 as follow [1]:

$$T_{\mathrm{lead1}\to\mathrm{lead2}}(E_{\mathrm{r}}) = \lim_{E_{\mathrm{i}}\to 0} \mathrm{Tr}\left[\Gamma_{\mathrm{lead2}}(E) G_{\mathrm{c}}(E) \Gamma_{\mathrm{lead1}}(E) \left(G_{\mathrm{c}}(E)\right)^{\dagger}\right], \tag{61}$$

where

$$\begin{aligned} G_{\mathrm{c}}(E) &= \frac{1}{E - \mathcal{H}_{\mathrm{eff}}(E)} \\ &\equiv \begin{pmatrix} G_{\mathrm{c}}(-n_0,-n_0) & \cdots & G_{\mathrm{c}}(-n_0,n_0) \\ \vdots & \ddots & \vdots \\ G_{\mathrm{c}}(n_0,-n_0) & \cdots & G_{\mathrm{c}}(n_0,n_0) \end{pmatrix}, \end{aligned} \tag{62}$$

$$\begin{aligned} \Gamma_{\mathrm{lead1}}(E) &\equiv i\left[\Sigma_{\mathrm{lead1}}(E) - \left(\Sigma_{\mathrm{lead1}}(E)\right)^{\dagger}\right] \\ &= \left(E_{\mathrm{i}} + \frac{\sqrt{E(E-4t)} + \sqrt{E^*(E^*-4t)}}{2}\right) \begin{pmatrix} 1 & 0 & \cdots & 0 \\ 0 & 0 & & \\ \vdots & & \ddots & \vdots \\ 0 & & \cdots & 0 \end{pmatrix}, \end{aligned} \tag{63}$$

$$\begin{aligned} \Gamma_{\mathrm{lead2}}(E) &\equiv i\left[\Sigma_{\mathrm{lead2}}(E) - \left(\Sigma_{\mathrm{lead2}}(E)\right)^{\dagger}\right] \\ &= \left(E_{\mathrm{i}} + \frac{\sqrt{E(E-4t)} + \sqrt{E^*(E^*-4t)}}{2}\right) \begin{pmatrix} 0 & \cdots & & 0 \\ \vdots & \ddots & & \vdots \\ & & 0 & 0 \\ 0 & \cdots & 0 & 1 \end{pmatrix}, \end{aligned} \tag{64}$$

with $E^* = E_{\mathrm{r}} + iE_{\mathrm{i}}$ being the complex conjugate of the energy E. The matrices in Eqs. (62)−(64) are all $(2n_0+1)\times(2n_0+1)$ matrices. The matrices (63) and (64) are necessary for the flux normalization. We thus obtain the transmission function as

$$T_{\mathrm{lead1}\to\mathrm{lead2}}(E_{\mathrm{r}}) = \left|\sqrt{E_{\mathrm{r}}(E_{\mathrm{r}}-4t)} G_{\mathrm{c}}(n_0,-n_0)(E_{\mathrm{r}})\right|^2. \tag{65}$$

Using the Landauer formula Eq. (2) for the transverse mode $M = 1$,

$$G(E_{\mathrm{r}}) = \frac{2e^2}{h} T_{\mathrm{lead1}\to\mathrm{lead2}}(E_{\mathrm{r}}), \tag{66}$$

we obtain the conductance of the conductor caused by a conduction electron flowing from lead 1 to lead 2.

We show in Fig. 20 the conductance for the three potentials in Sec. 6. We note that the peaks of the nonlinear conductance are caused by the resonant states.

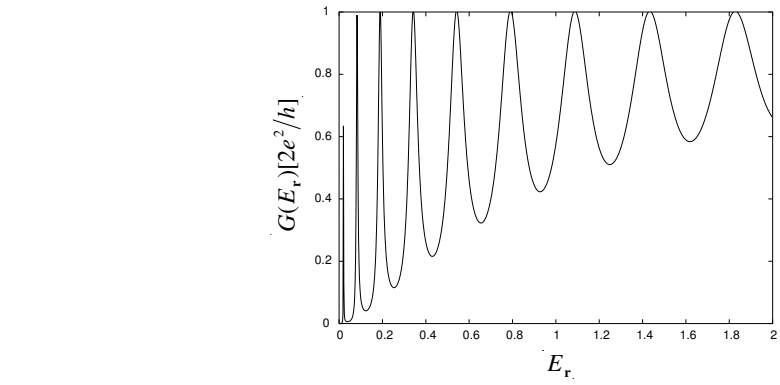

(a)

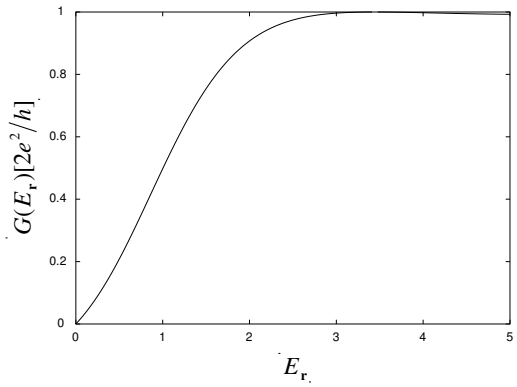

(b)

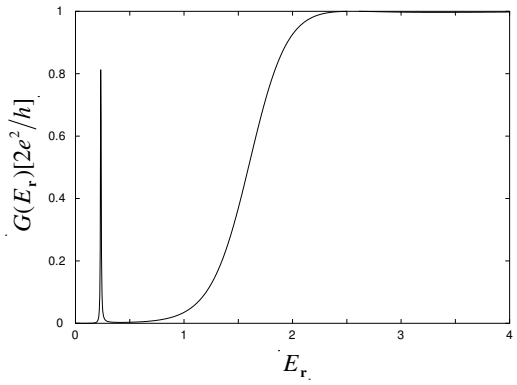

(c)

Figure 20: (a) The normalized conductance of the double delta potential in Subsec. 6.1. (b) The normalized conductance of the rectangular potential in Subsec. 6.2. (c) The normalized conductance of the double gaussian potential in Subsec. 6.3.

.

8 The case of many-body problem

In the present section, we try to treat a many-body problem by the present new method.

8.1 s-d exchange interaction

We first consider the Anderson Hamiltonian with interactions between conduction electrons and localized spins:

$$\begin{aligned} \mathcal{H} &= \sum_{k\sigma} \epsilon_k n_{k\sigma} + \sum_{\sigma} \epsilon_d n_{d\sigma} + U n_{d\uparrow} n_{d\downarrow} + \sum_{k\sigma} [V_{kd} c^\dagger_{k\sigma} c_{d\sigma} + V^*_{kd} c^\dagger_{d\sigma} c_{k\sigma}], \\ &= \mathcal{H}_0 + \mathcal{H}_1, \end{aligned} \tag{67}$$

where

$$\begin{cases} \mathcal{H}_0 &\equiv \sum_{k\sigma} \epsilon_k n_{k\sigma} + \sum_{\sigma} \epsilon_d n_{d\sigma} + U n_{d\uparrow} n_{d\downarrow} \\ \mathcal{H}_1 &\equiv \sum_{k\sigma} [V_{kd} c^\dagger_{k\sigma} c_{d\sigma} + V^*_{kd} c^\dagger_{d\sigma} c_{k\sigma}]. \end{cases} \tag{68}$$

The first term is the kinetic energy of the conduction electrons (the s-orbital electrons), the second term is that of the localized electrons (the d-orbital electrons), the third term is the Coulomb repulsive force between two electrons in the d-orbital, and the forth term is the hopping between the s-orbital and the d-orbital.

By using the Shcrieffer-Wolff transformation [5], we have

$$\mathcal{H} = \sum_{k\sigma} \epsilon_k n_{k\sigma} - \frac{J}{2N} \sum_{kk'\sigma\sigma'} c^\dagger_{k\sigma} \vec{\sigma}_{\sigma\sigma'} c_{k'\sigma'} \cdot \vec{S}_d. \tag{69}$$

The Fourier transformation yields

$$\begin{aligned} \mathcal{H} &= -t \sum_{i\sigma} \left(c^\dagger_{i+1\sigma} c_{i\sigma} + c^\dagger_{i\sigma} c_{i+1\sigma} \right) - J \vec{\sigma_0} \cdot \vec{S_0}, \\ &= \mathcal{H}_{\rm c} + \mathcal{H}_{\rm sd} \end{aligned} \tag{70}$$

where

$$\vec{\sigma_0} \equiv \frac{1}{2} \sum_{\sigma\sigma'} c^\dagger_{0\sigma} \vec{\sigma}_{\sigma\sigma'} c_{0\sigma'}. \tag{71}$$

Equation (70) is called the Kondo Hamiltonian (Fig. 21), where $\mathcal{H}_{\rm sd}$ denotes the exchange interaction between a localized spin at the origin and a conduction electron. We try to calculate resonant states of Eq. (70) by the present new method.

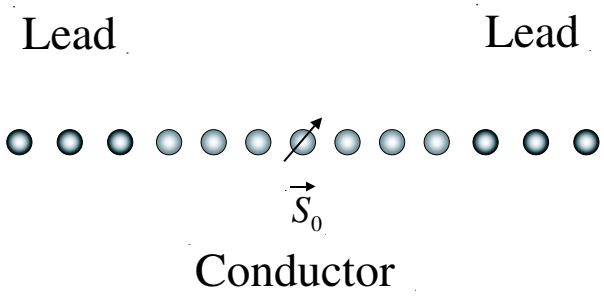

Figure 21: A conductor with a localized spin at the origin.

9 Conclusion

We propose a new method of treating open quantum systems with many-body interactions. We numerically calculated resonant states of various potentials. In Sec. 3, we showed that the resonant state generally has a diverging eigenfunction and a complex eigenvalue. In Sec. 4, we reduced the Hamiltonian of an infinite system into the effective one of a finite system, using the self-energy terms corresponding to the effects of the leads. The effective Hamiltonian of the finite system is non-Hermitian and energy-dependent, and hence it is hard to obtain its eigenvalue distribution by conventional methods. In Sec. 5, we introduced a new method of calculating the eigenvalue distribution of the effective non-Hermitian Hamiltonian. In Sec. 6, we demonstrated that eigenvalues of the resonant state obtained by the present new method agree with the exact solution. Thus we confirmed that the present method yields the exact eigenvalue and eigenfunction of one-electron models. In Sec. 7, we calculated the conductance of the three potentials in Sec. 6. We demonstrated that the resonant states largely affect the peaks of the nonlinear conductance. In Sec. 8, we try to apply the present method to a many-body problem (the *s*-*d* interaction).

Acknowledgements

I would like to express my gratitude to Associate Professor Naomichi Hatano for his helpful suggestions and discussions.

A The analysis of eigenvalues of Double delta potential

In the present appendix, we analyze the complex eigenvalues in the case of the double delta potential. We use the tight-binding model in order to obtain the complex wave number k.

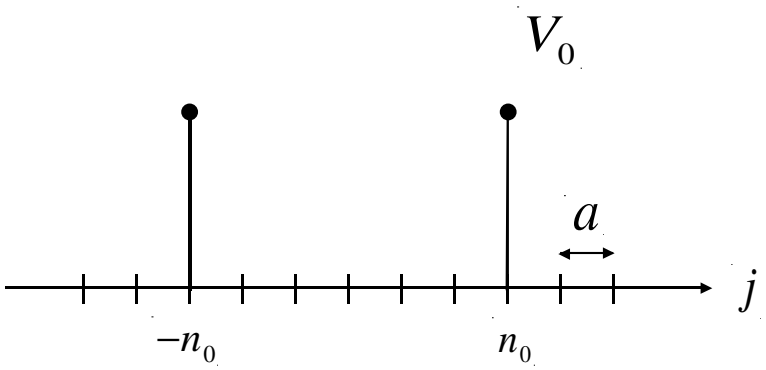

Figure 22: The double delta potential on a one-dimensional lattice model.

We can write down the solutions in each region of the potential immediately as follows:

$$\phi_j = \begin{cases} \mathcal{A}e^{-ikaj} & (j < -n_0), \\ \mathcal{B}e^{ikaj} + \mathcal{C}e^{-ikaj} & (j < |n_0|), \\ \mathcal{D}e^{ikaj} & (j > n_0), \end{cases} \tag{72}$$

where $\mathcal{A}, \mathcal{B}, \mathcal{C}, \mathcal{D}$ are generally complex coefficients. Here we choose only outgoing waves in the regions away from the potential, which is a boundary condition suitable for the resonant states [3]. Then we require the conditions that the wave functions are continuous at $j = \pm n_0$. Because of the symmetry $V_j = V_{-j}$, we expect solutions of a definite parity. Therefore, it is sufficient to apply the matching conditions to the solutions only at $j = n_0$. Now let us look for even solutions and odd solutions separately. For even solutions, we can set

$$\mathcal{A} = \mathcal{D}, \quad \mathcal{B} = \mathcal{C}. \tag{73}$$

Thus we rewrite Eq. (72) as follows:

$$\begin{cases} \phi_j^{\mathrm{I}} = \mathcal{D}e^{ikja} & (j > n_0), \\ \phi_j^{\mathrm{II}} = \mathcal{B}\left(e^{ikja} + e^{-ikja}\right) & (0 \le j < n_0). \end{cases} \tag{74}$$

At $j = n_0$, we obtain the relations between the wave functions as follows:

$$\begin{cases} \phi_{n_0}^{\mathrm{I}} = \phi_{n_0}^{\mathrm{II}}, \\ -t\phi_{n_0+1}^{\mathrm{I}} - t\phi_{n_0-1}^{\mathrm{II}} + (V_0 + 2t)\phi_{n_0}^{\mathrm{I}} = E\phi_{n_0}^{\mathrm{I}}. \end{cases} \tag{75}$$

Solving Eq. (75), we arrive at the conditional equation of even solutions:

$$1 - 2i\frac{t}{V_0}\sin ka = -e^{2ikn_0a}. \tag{76}$$

We can also obtain the odd wave functions in the same way. For odd solutions, we can set

$$\mathcal{A} = -\mathcal{D}, \quad \mathcal{B} = -\mathcal{C}. \tag{77}$$

Thus we rewrite Eq. (72) as follows:

$$\begin{cases} \phi_j^{\mathrm{I}} = \mathcal{D}e^{ikja} & (j > n_0) \\ \phi_j^{\mathrm{II}} = \mathcal{B}\left(e^{ikja} - e^{-ikja}\right) & (0 \le j < n_0). \end{cases} \tag{78}$$

At $j = n_0$, we obtain the relations between the wave functions as follows:

$$\begin{cases} \phi_{n_0}^{\mathrm{I}} = \phi_{n_0}^{\mathrm{II}} \\ -t\phi_{n_0+1}^{\mathrm{I}} - t\phi_{n_0-1}^{\mathrm{II}} + (V_0 + 2t)\phi_{n_0}^{\mathrm{I}} = E\phi_{n_0}^{\mathrm{I}}. \end{cases} \tag{79}$$

Solving Eq. (79), we arrive at the conditional equation of odd solutions:

$$1 - 2i\frac{t}{V_0}\sin ka = e^{2ikn_0a}. \tag{80}$$

We put Eqs. (76) and (80) together as follows:

$$1 - 2i\frac{t}{V_0}\sin ka = \pm e^{2ikn_0a}. \tag{81}$$

On the other hand, we obtain the dispersion relation by Eqs. (72) and (75) as follows:

$$E = 2t - 2t\cos ka. \tag{82}$$

We show in Table 1 the eigenvalues of resonant states in the case $V = 10$, $n_0 = 100$, and $a = 0.01$, computed using Mathematica.

n	eigenvalue	n	eigenvalue
1st	$0.0204727 - 0.000515478i$	6th	$0.787001 - 0.0616217i$
2nd	$0.0827563 - 0.00382655i$	7th	$1.08270 - 0.0854145i$
3rd	$0.188836 - 0.0115729i$	8th	$1.42714 - 0.111870i$
4th	$0.340714 - 0.0240931i$	9th	$1.82037 - 0.140594i$
5th	$0.539820 - 0.0409837i$	10th	$2.26241 - 0.171275i$

Table 1: The eigenvalues of resonant states for the double delta potential.

B The analysis of eigenvalues of Rectangular potential

In the present appendix, we analyze the complex eigenvalues in the case of the rectangular potential. We use the tight-binding model in order to obtain the relation equations for the complex wave numbers k and κ.

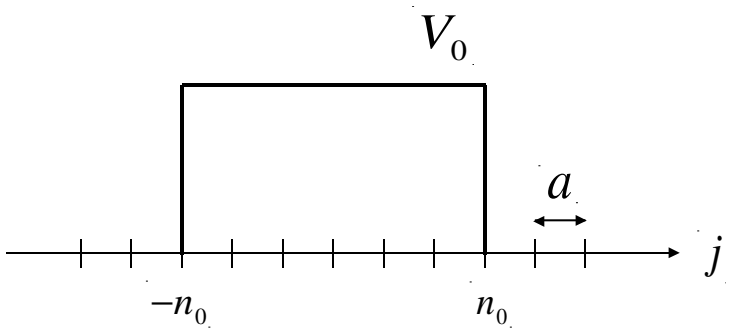

Figure 23: The rectangular potential on a one-dimensional lattice.

We can write down the solutions in each region of the potential immedi-

ately as follows:

$$\phi_j = \begin{cases} \mathcal{A}e^{-ika j} & (j < -n_0), \\ \mathcal{B}e^{i\kappa a j} + \mathcal{C}e^{-i\kappa a j} & (j < |n_0|), \\ \mathcal{D}e^{ika j} & (j > n_0), \end{cases} \tag{83}$$

where $\mathcal{A}, \mathcal{B}, \mathcal{C}, \mathcal{D}$ are generally complex coefficients. Here we choose only outgoing waves in the regions away from the potential, which is a boundary condition suitable for the resonant states [3].

Then we require the conditions that the wave functions are continuous at $j = \pm n_0$. Because of the symmetry $V_j = V_{-j}$, we expect solutions of a definite parity. Therefore, it is sufficient to apply the matching conditions to the solutions only at $j = n_0$. Now let us look for even solutions and odd solutions separately. For even solutions, we can set

$$\mathcal{A} = \mathcal{D}, \quad \mathcal{B} = \mathcal{C}. \tag{84}$$

Thus we rewrite Eq. (83) as follows:

$$\begin{cases} \phi_j^{\mathrm{I}} = \mathcal{D}e^{ikja} & (j > n_0), \\ \phi_j^{\mathrm{II}} = \mathcal{B}\left(e^{i\kappa j a} + e^{-i\kappa j a}\right) & (0 \le j < n_0). \end{cases} \tag{85}$$

At $j = n_0$, we obtain the relations between the wave functions as follows:

$$\begin{cases} \phi_{n_0}^{\mathrm{I}} = \phi_{n_0}^{\mathrm{II}}, \\ -t\phi_{n_0+1}^{\mathrm{I}} - t\phi_{n_0-1}^{\mathrm{II}} + (V_0 + 2t)\phi_{n_0}^{\mathrm{II}} = E\phi_{n_0}^{\mathrm{II}}. \end{cases} \tag{86}$$

Solving Eq. (86), we arrive at the conditional equation of even solutions:

$$1 + \frac{V_0}{t}e^{ika} = \frac{\cos\kappa(n_0 - 1)a}{\cos\kappa n_0 a}e^{ikn_0 a}. \tag{87}$$

We can also obtain the odd wave functions in the same way. For odd solutions, we can set

$$\mathcal{A} = -\mathcal{D}, \quad \mathcal{B} = -\mathcal{C}. \tag{88}$$

Thus we rewrite Eq. (83) as follows:

$$\begin{cases} \phi_j^{\mathrm{I}} = \mathcal{D}e^{ikja} & (j > n_0) \\ \phi_j^{\mathrm{II}} = \mathcal{B}\left(e^{i\kappa j a} - e^{-i\kappa j a}\right) & (0 \le j < n_0). \end{cases} \tag{89}$$

At $j = n_0$, we obtain the relations between the wave functions as follows:

$$\begin{cases} \phi^{\mathrm{I}}_{n_0} = \phi^{\mathrm{II}}_{n_0} \\ -t\phi^{\mathrm{I}}_{n_0+1} - t\phi^{\mathrm{II}}_{n_0-1} + (V_0 + 2t)\phi^{\mathrm{II}}_{n_0} = E\phi^{\mathrm{II}}_{n_0}. \end{cases} \tag{90}$$

Solving Eq. (90), we arrive at the conditional equation of odd solutions:

$$1 + \frac{V_0}{t}e^{ika} = \frac{\sin\kappa(n_0 - 1)a}{\sin\kappa n_0 a}e^{ikn_0 a}. \tag{91}$$

We put Eqs. (87) and (91) together as follows:

$$\begin{cases} 1 + \dfrac{V_0}{t}e^{ika} = \dfrac{\cos\kappa(n_0 - 1)a}{\cos\kappa n_0 a}e^{ikn_0 a} & \text{(even)}, \\ 1 + \dfrac{V_0}{t}e^{ika} = \dfrac{\sin\kappa(n_0 - 1)a}{\sin\kappa n_0 a}e^{ikn_0 a} & \text{(odd)}. \end{cases} \tag{92}$$

where wave numbers k and κ are the relation as follow :

$$\cos\kappa a - \cos ka = \frac{V_0}{2t}. \tag{93}$$

On the other hand, we obtain the dispersion relation by Eqs. (83) and (86) as follows:

$$E = 2t - 2t\cos ka. \tag{94}$$

We show in Table 2 the eigenvalues of resonant states in the case $V = 1, n_0 = 100$, and $a = 0.01$, computed using Mathematica.

n	eigenvalue	n	eigenvalue
1st	$0.821201 - 1.68808i$	6th	$74.6165 - 53.1537i$
2nd	$4.03060 - 9.24567i$	7th	$105.127 - 65.6679i$
3rd	$13.6555 - 18.9470i$	8th	$140.629 - 78.5869i$
4th	$28.7846 - 29.6646i$	9th	$181.088 - 91.8534i$
5th	$49.1457 - 41.1184i$	10th	$226.476 - 105.422i$

Table 2: Analysis of eigenvalues of the resonant state for the rectangular potential.

References

[1] S. Datta, Electronic Transport in Mesoscopic Systems (Cambridge University Press, Cambridge, 1995).

[2] B. J. van Wees, H. van Houten, C. W. J. Beenakker, J. G. Williamson, L. P. Kouwenhoven, D. van der Marel, and C. T. Foxon , Phys. Rev. Lett. **60**, 848 (1988).

[3] N. Hatano, Complex eigenvalues and resonant states (2003), unpublished.

[4] M. Embree and L. N. Trefethen, SIAM J. Sci. Comput. **23**, 583 (2001).

[5] J. R. Shcrieffer and P. A. Wolff, Phys. Rev. **149**, 491 (1966).